Sensitive Detection of Nonlinear Nanomechanical Motion Using Capacitive Signal Downmixing for Resonant NEMS Based Sensors

N. Kacem*, M. Sworowski**, S. Hentz**, S. Baguet*** and R. Dufour***

* FEMTO-ST, UMR 6174, CNRS-UFC-ENSMM-UTBM
24 chemin de l'Epitaphe F-25000 Besançon, France, najib.kacem@femto-st.fr
** CEA/LETI-MINATEC
*** Université de Lyon, CNRS INSA-Lyon, LaMCoS UMR 5259

ABSTRACT

We have developed a method of measuring resonance properties of high frequency nanoelectromechanical resonators for inertial sensor applications based on capacitive downmixing. The technique takes advantage of the electrostatic actuation of the resonator to use it as a mixer. It also greatly reduces the effect of the cross-talk between the detector and actuator circuits. We achieve the detection of few nanometers oscillations and capacitance variations of few attoFarads of doubly clamped beam resonance up to $13.5\,MHz$ at room temperature, demonstrating that downmixed capacitive signal detection is a viable high-sensitivity method of displacement detection in high-frequency NEMS.

Keywords: nanoelectromechanical systems, nonlinear dynamics, resonant sensors, capacitive downmixing

1 INTRODUCTION

Nanoelectromechanical systems (NEMS) are emerging as strong candidates for a host of important applications in semiconductor-based technology and fundamental science [1]. At this level, the electric characterization of such nanoelectromechanical force sensor is a challenge. In fact, the high-frequency signals are normally cut off due to the limited bandwidth of the readout circuitry dominated by stray capacitance between the large amplifier and the high impedance tunneling junction. Some methods have been suggested to solve this problem: using several amplifier stages instead of a single transimpedance amplifier [2], inserting an LC resonator to transform down the tunneling junction resistance [3], employing pump-probe techniques [4], [5] or more recently the scanning tunneling microscopy downmixing readout technique [6].

In this paper, a new technique for the electrical characterization of capacitive NEMS resonators has been developed in order to overcome the problems of parasitic impedances at high frequency. Our technique utilizes two AC signals and the intrinsic properties of the resonator to perform heterodyne downmixing of the signal to a much lower frequency, which can then be detected by standard circuitry without significant signal loss. Not only does this increase the detected signal, it also greatly reduces unwanted background from the cross-talk between the detector and actuator circuits. The measurements are performed on the sensing part of a typical M&NEMS accelerometer, which has been designed and fabricated in order to validate our characterization method. This technique permits tuning the signal to nonlinearity ratio and sensing the nonlinear nanomechanical motion in high-frequency resonators.

2 DEVICE AND PROCESS FLOW

In order to improve the performances of micromachined resonant accelerometers, MEMS and NEMS technologies have been used on the same device. The proof mass was patterned at a MEMS level to keep sufficient inertial force while the unique NEMS part is a very sensitive sub-μm suspended resonator. The M&NEMS technology is based on SOI substrate, with a silicon top layer thickness equal to the NEMS resonator thickness. The process flow starts with the lithography and etching of the NEMS resonator and of the bulk contact. Then a $0.3\,\mu m$ thick oxide deposition followed by a lithography and etching of the nanoresonator protection are proceeded. In the same step, an over etching of the oxide is led to open the silicon bulk contact. A few microns thick silicon epitaxial growth is done to realize the MEMS part. Depending on the silicon doping level of the MEMS part, an implantation step can be added for the electrical contact pads. Contacts are defined by a $0.5\,\mu m$ metal deposition followed by a lithography and etching of pads. A last lithography step and a DRIE of silicon thick layer is proceeded to make the MEMS structure, to isolate the bulk contact, and to open the SiO2 protective layer of the NEMS. The release of the sensor then is achieved by HF-vapor etching. Using the presented flow, with the 6 mask levels of the M&NEMS technology, a first high-g accelerometer was designed and fabricated in the 8" silicon platform of the LETI. For that proof of concept device, the resonator was limited to $0.250.5\,\mu m^2$ section, and the MEMS thickness was reduced to $2\,m$ thick. The total area of the accelerometer is less than $0.1\,mm^2$. SEM image of an in-plane M&NEMS accelerometer is shown in Figure 1.

The critical part in the designed accelerometer is the

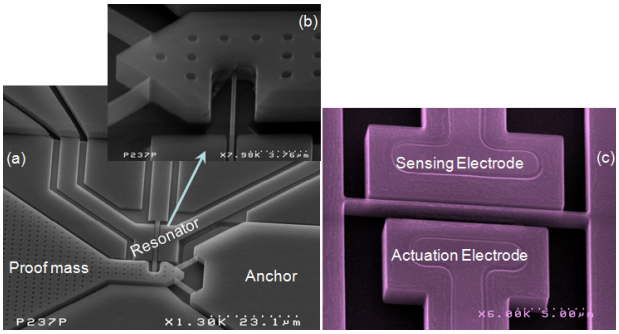

Figure 1: (a): SEM view of an in-plane M&NEMS accelerometer. (b): A focus on the gauge lets clearly appear the MEMS inertial mass of $2\,\mu m$ thick, and the sub-μm resonator that has a section of $0.250.5\,\mu m^2$. (c): A SEM image of a designed nanoresonator.

resonator which has been fabricated at the NEMS level ($500\,nm$ thick) with frequencies in the MHz range. Indeed, the smaller the structure the sooner nonlinearities occur [7]–[11] and the read out capacitive signal bellow the critical amplitude (few nanometers) is very low (few attofarad). Combined with the parasitic impedance cross-talk issues at high frequencies which changes the expected behavior of the electrical circuit, this makes the characterization of such devices complicated. It is then a challenge to find the adequate electrical measurement technique for the dynamic characterization of these nanoelectromechanical resonators.

3 CAPACITIVE DOWNMIXING

3.1 Principle

The downmixing technique has been widely used in NEMS read-out to avoid high frequency problems by making measurements at a lower frequency through synchronous lock-in methods [12]–[14]. A working principle schematic is shown in Figure 2. A periodic electrostatic force is generated between the actuation electrode and the clamped-clamped beam in order to enable the oscillation of the resonator at its first bending mode shape which corresponds to the first harmonic (the primary resonance at the frequency ω). Moreover, the beam is polarized using a periodic voltage which corresponds to the second harmonic at the frequency $\omega + \Delta\omega$. Consequently and due to the NEMS mixing, a capacitance variation is generated between the beam and the detection electrode at a low frequency harmonic $\Delta\omega$. Thus, the created low motional current at the frequency $\Delta\omega$ is detected using a lock-in amplifier (LIA). The latter needs a reference signal, which is created thanks to an RF mixer in order to track the resonance peak at the low frequency $\Delta\omega$.

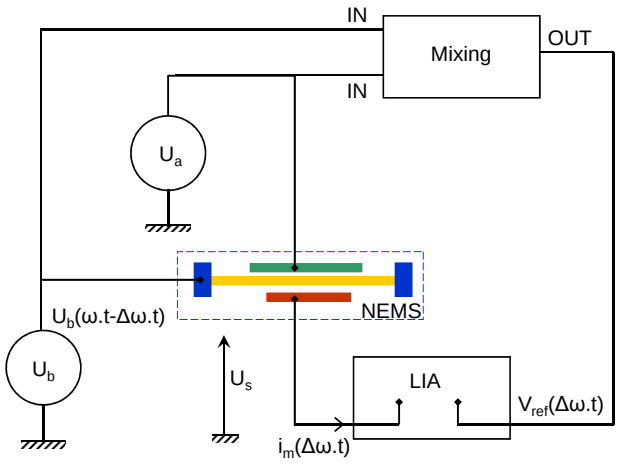

Figure 2: A working principle schematic of a capacitive downmixing setup.

3.2 Configurations

The current I_{out} between the resonator and the detection electrode is converted into the tension V_{out} due to an equivalent impedance that corresponds to the cable capacitance ($\approx 100\,pF$) in parallel with the lock-in input impedance (a capacitance of $25\,pF$ in parallel with a resistance of $10\,M\Omega$). For a frequency $> 1\,KHz$, the equivalent impedance is reduced to the capacitance due to the cables and the lock-in input $Z_{load} \approx C_{load} \approx 125\,pF$. Under the effect of the electrostatic forces applied to the beam, we consider that the resonator vibrates on its first mode at the frequency ω close to its primary resonance ω_0. We consider also the phase φ which can exist between the vibration of the beam and the harmonic ω of the actuation force. At resonance, the beam displacement is $w(t)$ and the capacitance between the beam and the detection electrode is assumed to be:

$$C_d(\omega t) \approx C_{0d}\left(1 + w(t).\cos(\omega t + \varphi)\right) \tag{1}$$

The current I_{out} is then:

$$I_{out} = \frac{dQ}{dt} = (U_b - U_s)\frac{dC_d}{dt} + C_d\frac{d\,(U_b - U_s)}{dt} \tag{2}$$

We assume that $V_b >> V_s$, hence:

$$\begin{aligned} I_{out}(t) &= U_b\frac{dC_d}{dt} + C_d\frac{dU_b}{dt} \\ &= \left(\omega - \frac{\Delta\omega}{2}\right).C_{0d}.w(t).V_b\sin\left(2\omega t - \Delta\omega t + \varphi\right) \\ &\quad + (\omega - \Delta\omega).C_{0d}.V_b\sin\left(\omega t - \Delta\omega t\right) \\ &\quad + \frac{\Delta\omega}{2}C_{0d}.w(t).V_b\sin\left(\Delta\omega t + \varphi\right) \end{aligned} \tag{3}$$

The measured voltage via the LIA is then:

$$U_{out} = Z_{load}.I_{out} = \frac{R_{load}.Iout}{1 + jR_{load}C_{load}\omega} \quad (4)$$

For $\omega >> \omega_{load} = \frac{1}{R_{load}C_{load}}$,

$$U_{out} \approx \frac{I_{out}}{jC_{load}\omega} \quad (5)$$

$$U_{out}^{\Delta\omega} \approx \frac{I_{out}^{\Delta\omega}}{jC_{load}\Delta\omega} \approx \frac{\frac{\Delta\omega}{2}C_{0d}.w.V_b \sin(\Delta\omega t + \varphi)}{jC_{load}\Delta\omega}$$
$$\approx j\frac{C_{0d}}{2C_{load}}.w(t).V_b.\ sin(\Delta\omega t + \varphi) \quad (6)$$

$$||U_{out}^{\Delta\omega}|| \approx j\frac{C_{0d}}{2C_{load}}.w.V_b = V_{out} \quad (7)$$

The beam displacement w depends on the electrostatic forces. In order to simplify the following analysis, only the actuation force is considered. Then, the electrostatic force can be written as:

$$||F_{elec}||_\omega = \frac{C_n}{2}\epsilon_0.b.l\left|\left|\frac{(U_a - U_b)^2}{(g_a - w)^2}\right|\right| \quad (8)$$

This electrostatic force depends on the actuation voltage U_a. Three different configurations have been identified:

- Ω configuration: $U_a = V_{dc} + V_a\cos(\omega t)$ and the excitatory harmonic is proportional to $2V_aV_{dc}$.
- 2Ω configuration: $U_a = V_a\cos(\frac{\omega}{2}t)$ and the excitatory harmonic is proportional to $\frac{1}{2}V_a^2$.
- V_aV_b configuration: the actuation voltage is:

$$U_a = V_a\cos(2\omega t - \Delta\omega t) \quad (9)$$

Hence:

$$(U_a - U_b)^2 = -V_a.V_b\cos(\omega t) + \frac{1}{2}V_a^2$$
$$+\frac{1}{2}V_b^2 - V_a.V_b\cos(3\omega t - 2\Delta\omega t)$$
$$+\frac{1}{2}V_a^2\cos(\frac{4\omega}{2}t - 2\Delta\omega t)$$
$$+\frac{1}{2}V_b^2\cos(2\omega t - 2\delta\omega t) \quad (10)$$

The first term on the right hand side of Equation (10) is the excitatory harmonic which is proportional to V_aV_b.

$$||(U_a - U_b)^2||_\omega = V_aV_b \quad (11)$$

4 EXPERIMENTS

For the sake of simplicity, several resonators designed for the considered M&NEMS accelerometer have been fabricated as isolated structures in order to validate the capacitive downmixing on high frequency NEMS. After some tests on the three capacitive downmixing categories, the last configuration (V_aV_b) has been chosen for the electrical characterization of NEMS resonators electrostatically actuated. Compared to Ω and 2Ω configurations, the last configuration gives the highest background to signal ratio (SBR) (low V_a and high V_b) while it keeps a low noise level ($20 - 30\,nV$).

The considered device under test is shown in Figure 1(c). It is $15\,\mu m$ long, $500\,nm$ thick, $400\,nm$ wide, the actuation gap is $1\,\mu m$, and the detection gap is $250\,nm$. It was placed in a vacuum chamber and measurements were performed at room temperature.

4.1 Linear Behavior

Figure 3 shows two linear resonance peaks obtained by capacitive downmixing (V_aV_b configuration) for an actuation voltage of $50\,mV$. The experimental resonance frequency is around $13.5\,MHz$. The negative frequency shift with respect to the theoretical frequency ($15.6\,MHz$) is due to the residual compression stress combined with the fabrication defects and the variation of the Young modulus for silicon nanostructure.

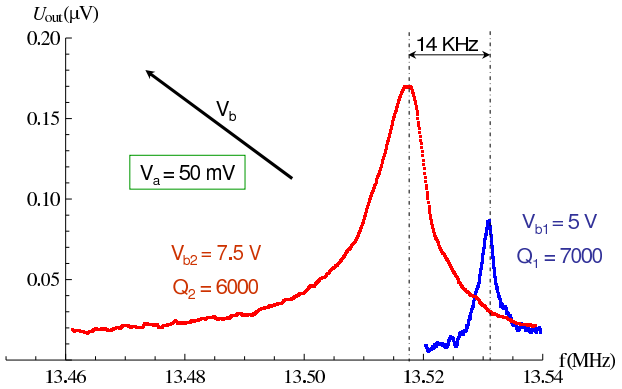

Figure 3: Linear resonance peaks experimentally measured using the V_aV_b capacitive downmixing technique.

Remarkably, The experimental setup enables the detection of very low capacitance variations (the static capacitances are $C_{0a} = 40\,aF$ in actuation and $C_{0d} = 210\,aF$ in detection) as demonstrated by the curve at the right where the output voltage is below $100\,nV$ for a bias voltage $V_b = 5\,V$ and the measured quality factor is around 7000. When the bias voltage is increased from $5\,V$ to $7.5\,V$, the frequency is shifted by $14\,KHz$ due to the negative electrostatic stiffness proportional to V_b^2 (for $V_a << V_b$). The dynamic bending deflection

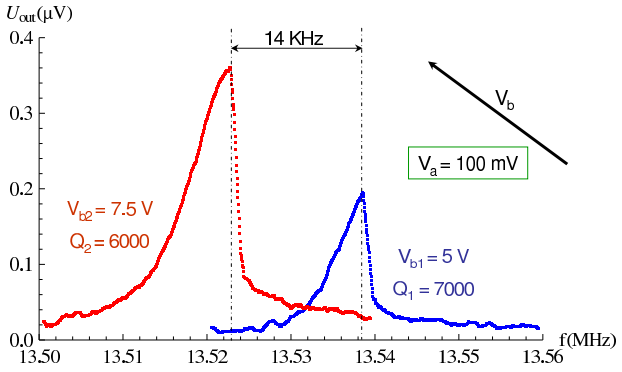

Figure 4: Nonlinear hardening resonance peaks experimentally measured using the $V_a V_b$ capacitive downmixing technique.

of the beam $w(x,t)$ is proportional to V_b, V_a as well as the quality factor. Moreover, the output voltage V_{out} is proportional to V_b and $w(x,t)$. Therefore, for a given drive voltage, the output voltage is proportional to the product $Q.V_b^2$. Obviously, for a bias voltage of $7.5\,V$, the ohmic losses [15] significantly increase and consequently, the quality factor decreases from 7000 down to 6000. The ratio between the two peaks amplitudes is around 1.9 which is approximately equal to $\frac{Q_2.V_{b2}^2}{Q_1.V_{b1}^2}$.

4.2 Nonlinear Behavior

Figure 4 shows two nonlinear hardening frequency responses measured on the same nanoresonator at an actuation voltage of $100\,mV$. The peak at the right is close to the critical amplitude A_c, even if the output voltage is about $200\,nV$ which is close to the amplitude of the linear peak at the left in Figure 3.

Since the dynamic bending deflection of the beam $w(x,t)$ is proportional to V_a and the quality factor, the increase of the drive voltage (for a given bias voltage) amplifies proportionally and purely mechanically the output voltage V_{out}. However, for a given drive voltage, the increase of the bias voltage amplifies mechanically and electrically the output signal. Hence, in order to maximise the output voltage while keeping a linear behavior, the use of very high bias voltage with respect to the drive voltage is recommended. The analytical critical amplitude [7] of the considered resonator is around $10\,nm$ which corresponds approximately to the oscillation amplitude of the beam in the curve on the right hand side of Figure 4. Consequently, the resonator oscillation is below $5\,nm$ for the smallest measured peak of Figure 3 which confirms the high sensitivity of the experimental setup for the capacitive detection of few nanometers of motion. The curve at the left in Figure 4 displays a hardening behavior beyond the critical mechanical amplitude of the resonator for a bias voltage of $7.5\,V$. The frequency shift between the two peaks of $14\,KHz$ due to the negative stiffness is maintained like in the linear case.

5 CONCLUSIONS

In this paper, a high-g M&NEMS accelerometer has been designed and fabricated. Its sensing part, a high frequency NEMS resonator, has been electrically characterized using a very sensitive capacitive downmixing set-up allowing the tuning of the signal to nonlinearity ratio and the detection of resonator motions below $5\,nm$. In a future work, the nonlinear dynamics of the considered sensor will be modeled while taking into account the downmixing characterization scheme. Experimental and model results will be compared, which will complete the experimental interpretations and finally improve the presented set-up.

REFERENCES

[1] M. L. Roukes, Phys. World, 14, 25, 2001.

[2] H. J. Mamin, H. Birk, P. Wimmer and D. Rugar, Journal of Applied Physics, 75, 161–168, 1994.

[3] U. Kemiktarak, T. Ndukum, K. C. Schwab and K. L. Ekinci, Nature, 50, 85–88, 2007.

[4] S. Loth, M. Etzkorn, C. P. Lutz, D. M. Eigler and A. J. Heinrich, Science, 329, 1628–1630, 2010.

[5] G. M. Steeves, A. Y. Elezzabi and M. R. Freeman, Applied Physics Letters, 70, 1909–1911, 1997.

[6] M. R. Kan, D. C. Fortin, E. Finley, K. M. Cheng, M. R. Freeman and W. K. Hiebert, Applied Physics Letters, 97, 253108, 2010.

[7] N. Kacem, S. Hentz, D. Pinto, B. Reig and V. Nguyen, Nanotechnology, 20, 275501, 2009.

[8] N. Kacem and S. Hentz, Applied Physics Letters, 95, 183104, 2009.

[9] N. Kacem, J. Arcamone, F. Perez-Murano and S. Hentz, Journal of Micromechanics and Microengineering, 20, 045023, 2010.

[10] N. Kacem, S. Baguet, S. Hentz and R. Dufour, International Journal of Non-Linear Mechanics, 46, 532–542, 2011.

[11] N. Kacem, S. Baguet, R. Dufour and S. Hentz, Applied Physics Letters, 98, 193507, 2011.

[12] I. Bargatin, E. B. Myers, J. Arlett, B. Gudlewski and M. L. Roukes, Applied Physics Letters, 86, 133109, 2005.

[13] C. Chen, S. Rosenblatt, K. I. Bolotin, W. Kalb, P. Kim, I. Kymissis, H. L. Stormer, T. F. Heinz and J. Hone, Nature Nanotechnology, 4, 861–867, 2009.

[14] V. Sazonova, Y. Yaish, H. Üstünel, D. Roundy, T. A. Arias and P. L. McEuen, Nature, 431, 284–287, 2004.

[15] V. Sazonova, "A Tunable Carbon Nanotube Resonator", Ph.D. thesis, Cornell University, 2006.